2023

Calibration of Perfluorinated Alkyl Acid Uptake Rates by a Tube Passive Sampler in Water

Matthew Dunn
University of Rhode Island

Jitka Becanova
University of Rhode Island, becanova@uri.edu

Jarod Snook
University of Rhode Island

Bridger Ruyle

Rainer Lohmann
University of Rhode Island, rlohmann@uri.edu

Citation/Publisher Attribution

Dunn, M., Becanoca, J., Snook, J., Ruyle, B. & Lohmann, R. (2023). Calibration of Perfluorinated Alkyl Acid Uptake Rates by a Tube Passive Sampler in Water. *ACS EST Water, 3*(2), 323-341. https://doi.org/10.1021/acsestwater.2c00384
Available at: https://doi.org/10.1021/acsestwater.2c00384

Calibration of Perfluorinated Alkyl Acid Uptake Rates by a Tube Passive Sampler in Water

Calibration of Perfluorinated Alkyl Acid Uptake Rates by a Tube Passive Sampler in Water

Matt Dunn[1], Jitka Becanova[1], Jarod Snook[1], Bridger Ruyle[2], Rainer Lohmann[1,*]

[1] Graduate School of Oceanography, University of Rhode Island, 215 South Ferry Rd, Narragansett, 02882 RI, USA

[2] Harvard John A. Paulson School of Engineering and Applied Science, Harvard University, Cambridge, MA, USA,

[*] Corresponding author: Email: rlohmann@uri.edu; Tel (401)874-6612

Abstract

Per- and polyfluoroalkyl substances (PFAS) are a group of 4000+ man-made compounds of great concern due to their environmental ubiquity and adverse effects. Despite a general interest, few reliable detection tools for integrative passive sampling of PFAS in water are available. A microporous polyethylene tube with a hydrophilic-lipophilic balance sorbent could serve as a flow-resistant passive sampler for PFAS. The tube's sampling rate, Rs, was predicted based on either partitioning and diffusion, or solely diffusion. At 15 ℃, the laboratory measured Rs for perfluorohexanoic acid of 100+/-81 mL day^{-1} were better predicted by a partitioning and diffusion model (48+/-1.8 mL day^{-1}) across 10-60 cm s^{-1} water flow speeds (15+/-4.2 mL day^{-1} diffusion only). For perfluorohexane sulfonate, Rs at 15 ℃ were similarly different (110+/-60 mL day^{-1} measured, 120+/- 63 versus 12+/-3.4 mL day^{-1} in respective models). Rs values from field deployments were in-between these estimates (46 +/-40 mL day^{-1} for perfluorohexanoic acid). PFAS uptake was not different for previously biofouled membranes in the laboratory, suggesting the general applicability of the sampler in environmental conditions. This research demonstrates that the polyethylene tube's

sampling rates are sensitive to the parameterization of the models used here and partitioning-derived values should be used.

Key Words:

PFAS, Passive Sampling, Sampling Rate, Numerical Model, Environmental Monitoring, PFHxA, PFHxS

Synopsis:

A tube passive sampler design was investigated for deriving sampling rates of nine PFAA with good agreement between measurements in the laboratory, field, and model derived values.

1. Introduction

Per- and polyfluorinated alkyl substances (PFAS) are a group man-made compounds that have been identified as contaminants of emerging concern. For decades, PFAS have been used in the production of fluoropolymers, water and stain proof surfaces, non-stick cookware, food contact materials, and aqueous film forming foams (AFFF) used to fight hydrocarbon fires.[1,2,3,4] Several PFAS pose a wide range of adverse human health impacts due to their ability to bioaccumulate, persist, and be passed on from mother to infant.[5,6] PFAS have been ubiquitously detected in environmental matrices including drinking water, biota, sediments, air, and human serum.[7,8,9,10,11,12] Specific human health effects include negative impacts on immune system response, obesity and high cholesterol risks, and increased tumor incidence associated with specific cancers.[5] Some PFAS, most notably perfluorooctanoic acid (PFOA) and perfluorooctane sulfonic acid (PFOS) have been phased out from production in the US and in the European Union.[4,13] However, the United States' current regulations are narrowly focused on PFOA and PFOS despite the potential occurrence of over 4000 PFAS compounds of variable chemistry, in contrast to the European Union's attempt to eliminate the use of additional PFAS.[13,14,15]

Concerns over the presence and effects of PFAS have increased the need for affordable and reliable tools for monitoring and investigating environmental PFAS contamination. Passive sampling is a low-cost alternative to traditional (active) water grab sampling that requires no power source for in-situ deployments.[16,17] The unique chemistry of PFAS makes most traditional equilibrium-based passive sampling technology not applicable for monitoring ionic PFAA in water. Instead, existing passive samplers for PFAS are typically operating in linear uptake as integrative samplers, such as the polar organic chemical integrative sampler (POCIS) design.[18,19,20,21,22] To reduce the impact of flow on uptake reported in studies using POCIS, we tested a passive sampler with a thicker membrane first introduced for passive sampling of glyphosate, aminomethyl phosphonic acid (AMPA), and PFAS in groundwater.[19,23,24,25,26,27] This tube passive sampler possesses a 0.2 cm thick microporous high density polyethylene (HDPE) membrane in contrast to the 0.014 cm thick membranes reported for POCIS deployments.[23,24]

Integrative samplers report time weighted averages of water concentrations that can give a more representative depiction of surface water contamination across diurnal, tidal, and seasonal trends than discrete grab sampling.[18,24,27,28,29,30,31] Other passive sampler designs such as the diffusive gradient in thin film (DGT) samplers have been investigated for PFAS in surface waters.[32,33,34,35] Recently, an equilibrium-based sampler for PFAS was investigated, using modified nanographene hydrogel to create a water-based sampler as opposed to sorbent-based sampler.[36] This study was hence performed to calibrate and validate an integrative passive sampler based on a microporous polyethylene tube sampler filled with sorbent for the accumulated of dissolved PFAS in surface waters.

Integrative passive samplers require a thorough understanding of sampling rates (R_s, volume per time) that relate the accumulated mass of the target compounds to environmental concentrations. The transfer of analyte from water into the sampler can be described (see Equation 1) using the overall mass transfer (k_0) of a dissolved polar organic compound separated into three main steps: mass transfer through the water boundary layer (k_w), transfer through the membrane (k_m), and finally through the sorbent (k_s) with units of velocity for all three transfers:

$$\frac{1}{k_0} = \frac{1}{k_w} + \frac{1}{k_m K_{mw}} + \frac{1}{k_s K_{sw}} \text{ (eqn 1),}$$

where K_{mw} is the partitioning constant (g water per g HDPE) for a given compound between the membrane and water, and

K_{sw} is the partitioning between the sorbent and water (g water per g sorbent).[17,20, 32, 34,35]

This model can be adjusted to reflect the unique chemistry of each PFAS, and the properties of the microporous membrane and sorbent used in the tube passive sampler for PFAS. The use of a thick membrane suggests that resistance through this barrier will dominate uptake kinetics.[37] The transport through the water boundary layer (k_w) can be estimated using a numerical approach recently published.[38] This numerical method was used to estimate k_m and k_s based on the thickness of each barrier and the diffusion through each barrier[27]. The latter diffusion was calculated as the aqueous diffusivity multiplied by the porosity of the barrier. We assume that all diffusion transport is through the pore spaces of the membrane and sorbent, with only adsorption processes as opposed to absorption.

While we assume that mass transfer is rate-limited by diffusion across the membrane, not the sorbent layer, both terms are retained in the equation to verify this.[37] Equation 1 is then rearranged, with the k_s and k_m terms substituted as follows (eqn 2):

$$\frac{1}{k_0} = \frac{1}{k_w} + \frac{d_m}{K_{mw} * (D_w * \emptyset_m)} + \frac{d_{sbl}}{K_{sw} * (D_w * \emptyset_s)} \text{ (eqn 2)}$$

where D_w is the aqueous diffusion of a PFAS compound ($cm^2\ s^{-1}$),

$\emptyset$ is the porosity of the membrane ($\emptyset_m$) and sorbent ($\emptyset_s$, in %), and

d (cm) are the thicknesses of the membrane (d_m) and sorbent boundary layer (d_{sbl}).[27]

With this model, the sampling rate can be predicted, and investigated across many environmental parameters including water flow speed, water temperature, water viscosity, as well as physical parameters associated with sampler designs including membrane types and different sorbent choices using equation 3 where *A* (cm^2) is the total surface area of the tube passive sampler:

$$\frac{1}{R_s} = \frac{1}{k_0 * A} \text{ (eqn 3)}$$

Sampling rate (cm^3 $second^{-1}$) can then be used as the conversion between mass of a given PFAS compound accumulated within the sampler to the time weighted average concentration in the water during the deployment length (eqn 4):.

$$C_w = \frac{N_s}{(R_s * 86.4) * t} \text{ (eqn 4),}$$

Where C_w is the time weighted average water concentration (ng L^{-1}),
R_s is converted to L day^{-1}, by the conversion factor of 86.4
N_s is the mass of a PFAS compound measured in the sampler (ng), and
t is the length of the deployment (days).

Equation 4 can also be rearranged to calculate a sampling rate for experimentally deployed passive samplers with known water concentrations in a laboratory setting. The use of this simple adjusted model can be compared to a more recent derivation of the model that has been highlighted for use with disk-shaped samplers in the literature which provides a more detailed model for steady state conditions in the sorbent layer.[37]

$$\frac{1}{k_0} = \frac{1}{k_w} + \frac{d_m * {\tau_m}^2}{(D_w * \emptyset_m)} + \frac{d_{sbl} * {\tau_s}^2}{(D_w * \emptyset_s)} \text{ (eqn 5),}$$

where d_{sbl} is the assumed thickness of the sorbent boundary layer at steady state conditions, which is 0.33 * the half thickness of the sorbent,

τ_m is the tortuosity of the flow path through the membrane pore space, which is always assumed to be 1, and

τ_s is the tortuoisity of the flow path through the sorbent bed, which is assumed to be 1.3 from other sorbent modeling literature.[26]

Most prior work reported calculated sampling rates for PFAS by POCIS sampler.[25,33,,31] The use of a thick, polyethylene membrane could then be a favorable alternative to previously tested passive samplers, with a lower partitioning PFAS to the membrane, an increased duration of the linear uptake phase and a reduced flow dependency.[26]

In summary, the purpose of this study was to (i) validate the uptake of PFAS in the tube passive sampler in a tank under controlled laboratory conditions (ii) investigate the impacts of flow, temperature, and biofouling on the measured and modeled sampling rates of selected PFAS, and (iii) assess the performance of PFAS mass transfer modeling approaches from the literature for integrative passive samplers.

Materials & Methods

Chemicals and Reagents. Liquid chromatography-grade methanol (LC-MeOH), and water (LC-water) were purchased from Fisher Scientific (New Hampshire, USA) along with ammonium hydroxide (NH_4OH), ammonium acetate ($C_2H_7NO_2$), ACS-grade ethanol (EtOH) and ACS-grade methanol (MeOH). Analytical standards were used to create native compound standards from the Wellington PFAC-30PAR mix plus an additional four analytical compounds (Table S1). Mass labeled surrogate solutions were derived from Wellington Laboratories' MPFAC-30ES plus an additional three mass labeled compounds purchased from Wellington Laboratories (Canada). Standards with a range of purity (94-98%) were used to create spiking solutions for all laboratory experiments and consisted of 24 individual compounds purchased from Toronto Research Chemicals (Canada), SynQuest (Florida, USA), Apollo Scientific (United Kingdom), and Santa Cruz (Texas, USA) (S1).

Solutions were created from solid standards and diluted in LC-MeOH before being stored in the refrigerator while awaiting use. Only 9 PFAA compounds (the C4-C8 PFCA and the C4-C8 PFSA) have published aqueous diffusivities, an important parameter for the modeling of sampler uptake. These 9 PFAA were included in the twenty-four-mix spiked into the experimental apparatus and are the focus of this study. Two specific PFAA will be highlighted, PFHxA and PFHxS, as they have become broadly used in place of PFOA and PFOS and recently have been oft detected in environmental matrices; three additional PFAS compounds, two long chain (>C7) PFCA and one fluorotelomer sulfonate were also included in the study.

Passive Sampler Assembly. The assembly of the tube passive samplers for PFAS was based on the method outlined by Fauvelle et al, 2017.[23] Microporous polyethylene tubes purchased from the Pall Corporation (Filtroplast, 12 mm O.D., 8 mm I.D. 35% porosity, 2.5 um pore size, 0.6 g cm^{-3} density) were cut into 7 cm long sections. These 7 cm long tube sections were then submerged in a 24-hour EtOH wash which was followed by a 24-hour LC-MeOH wash. Once fully dry, one end of the tube was closed using a snap-in polyethylene cap purchased from McMaster Carr, and 600 mg of Oasis hydrophilic lipophilic balance (HLB) sorbent was measured out and poured inside the open end of the tube. HLB sorbent was chosen as opposed to weak anion exchange (WAX) due to its affinity for a wider range of chemistries aside from just anionic PFAS, which will be vital to future applications.[20] Prior to deployment in the laboratory, assembled tube samplers were conditioned for at least 24 hours in LC-MeOH, followed by 24-hours in LC-water. The tube samplers were then either immediately deployed into the laboratory, field, or stored in LC-water until the experiment began.

Passive Sampler Extraction. Immediately following deployment, the tube passive sampler was placed in a 15 mL Falcon Tube and centrifuged at 4000 rpm for 2 minutes using an Eppendorf Centrifuge 5810 (Fisher Scientific, USA) to remove any water remaining in the tube membrane or sorbent. This centrifugation step is repeated until no further water is collected in the bottom of the tube. At this point, the tube was either frozen for future extraction after a maximum of six months or extracted immediately using liquid solid extraction (LSE). Tube samplers were submerged in approximately 6 mL of LC-grade MeOH that had been spiked with a mass labeled surrogate standard (MPFAC-30ES+3) within a 15 mL Falcon tube. After 24 hours, this methanol extract was collected in a pre-labeled, pre-cleaned Falcon tube. The tube sampler was centrifuged as previously described to remove any additional LC-MeOH, which was added to the collected extract. The sampler was then extracted in another 6 mL of LC-grade MeOH, resulting in roughly 12 mL total of extract. The extract was concentrated to approximately 0.5 mL in total volume under a gentle stream of Nitrogen while heated to 35℃. An aliquot of this final concentrate was diluted with 4 mM Ammonium Acetate in water and prepared for analysis via liquid chromatography tandem mass spectrometry (LC/MS/MS)

Instrumental Analysis. LC/MS/MS analysis was performed at the University of Rhode Island on a Shimadzu Prominence liquid chromatograph (UFLC) coupled to SCIEX TripleQuad 5500 MS/MS operating in negative mode for all laboratory and most field samples. Field samples collected in on Cape Cod were analyzed at Harvard University using an Agilent 6460 Triple Quadrupole Liquid Chromatography-tandem Mass Spectrometer following the method in previous work.[37] For additional details on the operating conditions, quality assurance, and interlaboratory comparison data refer to Tables S7-S10 in the SI.

Experimental Tank Deployments and Measurements. To measure laboratory uptake and sampling rates, triplicate tube passive samplers were deployed at four different flow rates (0, 10, 20, and 60 cm s^{-1}) and two different temperatures (15℃ and 25℃). Each trial consisted of a 14-day deployment, where duplicate 50 mL water grab samples were taken at the beginning and end of each deployment to verify PFAS concentrations during deployments (Fig S3). Water samples were extracted and analyzed in accordance with methods detailed in literature and used to calculate sampling rates for corresponding individual passive samplers using equation 4.[36,39] For additional details on the experimental tank design and construction, see SI.

PFAS Uptake by HDPE Membranes and HLB Sorbent. As part of the validation process of this passive sampler design and model, partitioning was measured for PFAS between the microporous polyethylene membrane (K_{mw}) and water (K_{sw}). Two complementary approaches were used to quantify K_{mw} values reflecting different deployment conditions: (1) Batch experiments on a shaker table (low flow) were performed in conjunction with (2) deployments of membranes without sorbent in the experimental tank at high water flows. Batch experiments, with either sorbent or tube membranes without sorbent were deployed in bottles of LC-grade water spiked with a known concentration of PFAS compounds. K_{mw} trials were specifically important to understanding the uptake of PFAS into the sampler due to the predicted high resistance to uptake of the membrane phase. For additional details on the K_{sw} methods, see SI.

Uptake by Bio Fouled Tube Membranes. Field deployments might incur an additional resistance to uptake from biofouling that is not accounted for in most laboratory and model methods. Clean tubes were left in a riverine environment for one month to naturally bio foul. These tubes were then re-conditioned (as above) and deployed in the experimental tank alongside freshly prepared tubes at two similar temperatures and two distinct flow speeds (0 and 60 cm s^{-1}) to investigate potential interferences of biota and environmental detritus on uptake through the microporous membrane.

Field Deployments. Passive samplers were deployed in the field for 14-28 days at three locations, including AFFF-impacted groundwater (JBCC) and river (QR9) downstream of a former fire training area on Joint Base Cape Cod, MA (USA) and a river downstream of a historical textile mill in Westerly, RI (Pawcatuck). Groundwater deployments (n = 3) were conducted for 14 days in June 2021 in a previously characterized PFAS plume[40] where the average linear groundwater velocity is 0.0005 cm s^{-1}. River deployments occurred between October 2019 and September 2020 at QR09 (n = 9), and in May 2021 at Pawcatuck (n = 2). Grab samples of surface and groundwater were collected during deployment and/or recovery of passive samplers and extracted in the manner described in previous literature by either the University of Rhode Island or Harvard University.[36,39,41] For additional environmental and field QA/QC details, see SI.

Development of a Numerical Model. A correlation between aqueous diffusion coefficients for 5 PFCA at 20 ℃ reported by Schaefer et al. and the number of fluorinated carbons was used to derive best fit D_w values. These diffusivities were then applied to calculate mass transfer coefficients (MTC) through the water boundary layer, microporous membrane layer, and sorbent layer for each compound (eqn 2, eqn 5, Table S3).[42] We assumed that transport is entirely through the pore space of the microporous membrane and that the only diffusion within the sorbent layer is from aqueous diffusion within the water saturated interior, as in prior work.[32] Diffusion coefficients were adjusted to reflect the change in temperature in these experiments (15-25 ℃) using equation 6.[43]

$$\frac{D_{T1}}{D_{T2}} = \frac{T_1}{T_2} * \frac{v_{T2}}{v_{T1}} \text{ (eqn 6)}$$

Where *D* is the aqueous diffusivity at two given temperatures (*T1 and T2*),

And *v* is the dynamic viscosity of water at a given temperature.

Results & Discussion

Validation of tube passive sampler. Laboratory experiments were conducted to investigate the impact of temperature, flow rate, deployment length and biofouling on the sampling rates of the target PFAA by the PE-tube passive sampler. Sampling rates were calculated for laboratory and field observed samplers using equation 4. To be able to predicts sampling rates, laboratory experiments were completed to independently quantify PFAS sorption to the HDPE membrane and the HLB sorbent of the passive sampler. With those values, the predicted model sampling rates were then compared to the field and laboratory observed sampling rates.

Sampling Rates of PFAS by PE tube samplers in laboratory experiments. Sampling rates of PFAA by the tube passive sampler in the laboratory experiments increased with chain length. For example, for PFCA, average sampling rates across 10-60 cm s^{-1} water flow increased from PFBA (12 ± 6), to PFPeA (18 ± 5 mL day^{-1}) to PFHxA (120 ± 51 mL day^{-1}), and PFOA (120 ± 55 mL day^{-1}) at 25℃ . PFSA had higher overall sampling rates than PFCA but displayed the same trend in chain length between PFBS, PFHxS, and PFOS (Table 1). To assess the impact of environmental variables of these sampling rates, the influence of water velocity and temperature on sampling rates was investigated.

Table 1. Sampling Rates For 9 PFAA. Laboratory and field observed sampling rates for 9 PFAA compounds of interest compared to two different derivations of a model for predicting sampling rates at three temperatures for flow rates between 0.5-60 cm/s. All observed values display one standard deviation, all predicted models display the uncertainty associated with the predicted value in the same units. Lab observed sampling rates were derived from 14-day deployments while field observed were 21-32 days in length.

Compound	Temp ℃	Lab Observed Rs (mL day^{-1}) n = 3	Field Observed Rs (mL day^{-1}) n = 11	Field Observed Rs (Gardiner et al. 2022)	EQN 2 Rs Low K_{mw} (mL day^{-1})	EQN 2 High K_{mw} (mL day^{-1})	EQN 5 Rs (mL day^{-1})
PFBA	5		16 (±06)		3.7 (±1.3)	63 (±33)	14 (3.9)
	15	22 (±12)	11 (±05)	7.3 (±5.5)	5.1 (±1.8)	86 (±45)	19 (5.3)
	25	12 (±6)			6.7 (±2.3)	110 (±59)	25 (7.0)
PFBS	5		44 (±20)		2.9 (±1.0)	89 (±46)	13 (3.6)
	15	40 (±11)	67 (±24)	22(±7.9)	4.1 (±1.4)	120 (±63)	18 (5.0)
	25	100 (±57)			5.3 (±1.9)	160 (±83)	23 (6.4)
PFPeA	5		30 (±11)		2.9 (±1.0)	8.7 (±4.5)	13 (3.6)
	15	18 (± 5)	35 (±18)	12 (±2.9)	4.1 (±1.4)	12 (±6.2)	18 (5.0)
	25	45 (±7)			5.3 (±1.9)	16 (±8.3)	23 (6.4)
PFHxA	5		37 (±13)		3.6 (±1.3)	35 (±18)	11 (3.1)
	15	100 (±81)	46 (±40)	18 (±5.5)	5.0 (±1.8)	48 (±25)	15 (4.2)
	25	120 (±51)			6.6 (±2.3)	63 (±33)	19 (5.3)
PFHxS	5		55 (±28)		26 (±9.2)	89 (±46)	8.7 (2.4)
	15	94 (±31)	67 (±28)	23 (±10)	35 (±13)	120 (±63)	12 (3.4)
	25	200 (±72)			48 (±17)	160 (±83)	16 (4.5)
PFHpA	5		46 (±20)		2.9 (±1.0)	58 (±30)	8.7 (2.4)
	15	72 (±60)	59 (±15)	23(±7.0)	3.9 (±1.4)	79 (±41)	12 (3.4)
	25	200 (±130)			5.2 (±1.8)	100(±54)	16 (4.5)
PFHpS	5		41 (±23)		12 (4.1)	120 (60)	6.8 (1.9)
	15	100 (±110)	120 (±83)	17 (±2.5)	16 (±5.7)	160 (±82)	9.4 (2.6)
	25	280 (±110)			21 (±7.5)	210 (±110)	12 (3.4)
PFOA	5		41 (±19)		6.2 (±2.2)	37 (±19)	6.8 (1.9)
	15	62 (±16)	58 (±10)	23 (±5.1)	8.5 (±3.0)	52 (±27)	9.4 (2.6)
	25	120 (±55)			11 (±3.9)	68 (±35)	12 (3.4)
PFOS	5		38 (±22)		19 (±6.8)	190 (±100)	4.9 (1.4)

	15	400 (±160)	63 (±24)	23 (±7.5)	27 (±9.4)	260 (±130)	6.7 (1.9)
	25	290(±110)			35 (±12)	340 (±180)	8.8 (2.5)

Influence of water flow velocity on Rs. For PFHxA and PFHxS, sampling rates were not a function of flow rate between 10-60 cm s^{-1} for laboratory and field observed, or equation 2 modeled sampling rates (Fig 1). Observed sampling rates did also not change as a function of water flow for the other PFAS (Table 1). The lack of water flow effect on sampling rate extended down to 0.5 cm s^{-1} based on the model (eqn 2) for flow rates below the 10 cm s^{-1} limit of most handheld flow meters. A lower value of approximately 0.5 cm s^{-1} flow speed is predicted to result in similar sampling rates as those seen between 10-60 cm s^{-1} (Figure S4 and S5).

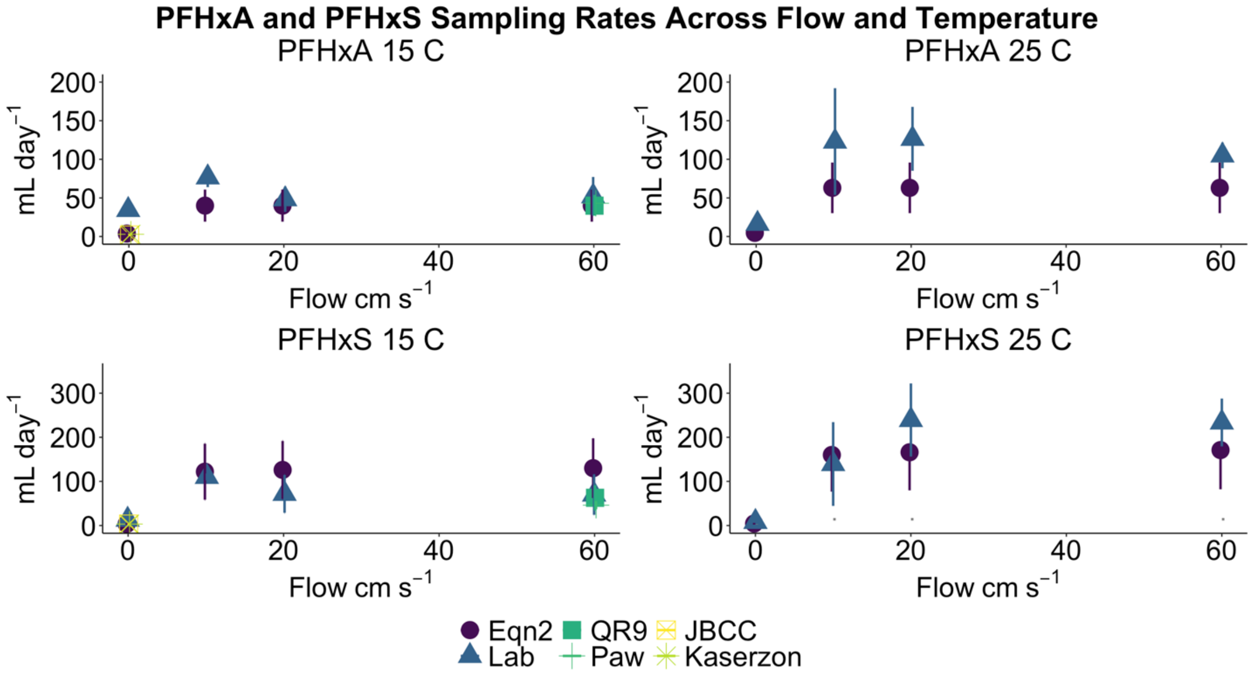

FIGURE 1. Modeled and observed sampling rates of PFHxA and PFHxS at two temperatures in the field deployments (15 ℃) and laboratory experiments (15 and 25 ℃). Error bars display 1 standard deviation for measurements and propagated uncertainty for modeling data. Figure includes previous groundwater deployments of this passive sampler by Kaserzon et al.[24]

Influence of temperature on Rs. The laboratory observed sampling rates increased for PFAA with increasing (10 ℃) temperature. The sampling rate increase with temperature for the tube passive sampler was greater for PFSA, on average by 46%, than for PFCA of similar chain length (Table 1, Fig 1, Fig S5). This increase is reflective of diffusivity's dependency on temperature, which was accounted for in the model development and application to accurately predict a 40% increase in sampling rate differences between 15 and 25 ℃. Additionally, the 25 ℃ laboratory observations exhibited a larger standard deviation in sampling rate amongst replicates than what as observed in the 15 ℃ or field observed sampling rates.

Uptake of PFAS by Biofouled tubes. To validate the performance of these passive samplers under field conditions, biofouling might introduce an additional resistance to uptake. There was no obvious difference between the mass of PFAS on clean and bio fouled tubes during concurrent laboratory experiments (Fig 2). This could be explained by considering how a thin, high water-content layer of algae, sponge, or other organic matter (Figure S8) compares to the thick polyethylene membrane in thickness and permeability[45,46]. However, biofouling conditions are very difficult to recreate in the laboratory, and the conditioning of these field-exposed tubes likely altered the biofouling layer. Further experiments, such as tube deployments in a laboratory setting with live algae/bacteria might be necessary to better assess the impact of biofouling on PFAS uptake.

To further explore this question, a fourth term was added to equation 2 to account for the uptake resistance introduced by a bio fouled membrane. We estimated the thickness of the biological layer to be 0.04 cm based on observation, and used reported K_{oc} values as a proxy for the affinity of PFAS to the organic material in the bio fouled layer:[47]

$$\frac{1}{k_0} = \frac{1}{k_w} + \frac{d_m}{K_{mw}*(D_w*\emptyset_m)} + \frac{d_s}{K_{sw}*(D_w*\emptyset_s)} + \frac{d_b}{K_{oc}*(D_w*\emptyset_b)} \quad \text{(eqn 7)}$$

The addition of the biofouled layer as parameterized above resulted in a 0.2-2% decrease in the modeled sampling rate for PFHxA and PFHxS at 15 and 25 ℃, which is insignificant when compared to the 52% uncertainty within the model. These considerations indicated the kinetic impact on sampling rate can be neglected when predicting sampling rate of a field deployed passive sampler, though physical issues such as pore blockage or sorbent congestion may remain a concern. Using the equation 7, a 1 cm thick layer of biofouling was calculated to be the limit at which the sampling rate would decrease by more than 25% for PFHxA and PFHxS at flow speeds >0.5 cm s^{-1}.

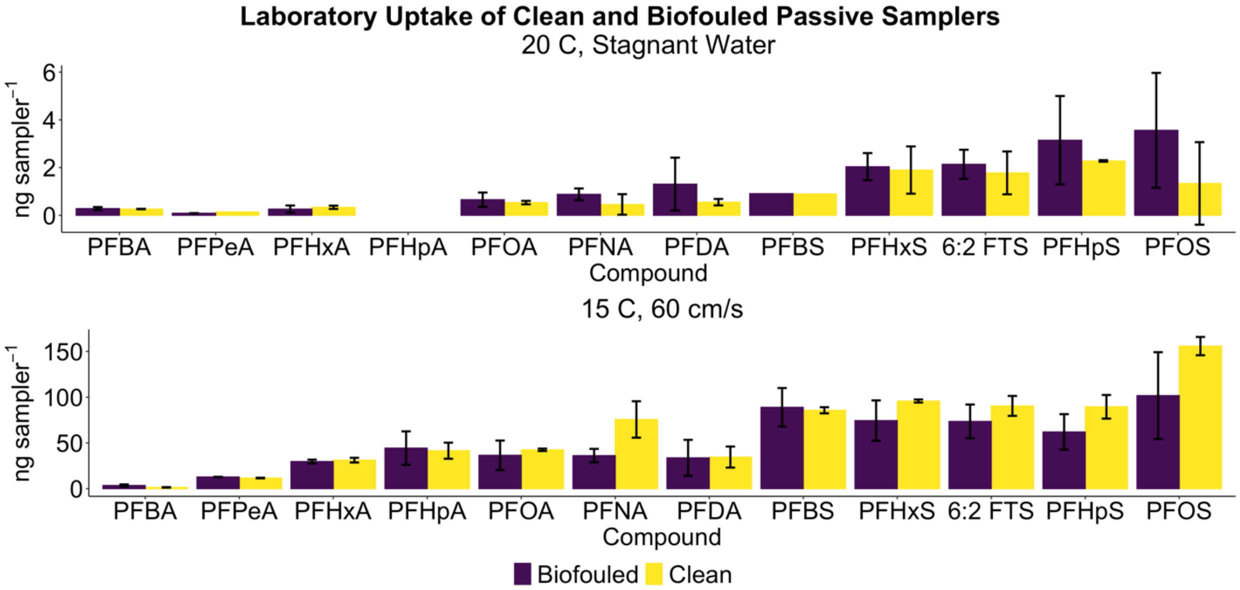

FIGURE 2. Comparison of mean PFAS mass (ng) measured in co-deployed tube samplers under similar conditions in the experimental tank. Error bars are 1 standard deviation of the mean.

Uptake of PFAS Over Time. Replicate passive samplers were deployed for 3, 7, 16, 28, and 54 days in the experimental tank to determine the length of time in which there is a net uptake of PFAS. The results suggest that linear uptake was maintained for most compounds between 0-16 days (Fig 3). As molecular weight increased, curvi-linear uptake and potential saturation at the sorbent/membrane interference by high molecular weight compounds was exhibited between 16 and 54 days (Fig 3). For example, uptake of PFDA, PFHpS, and PFOS seemed to cease, exhibiting no visible increase in mass after 16 days. PFPeA, PFHxA, PFHpA, PFOA, PFNA, PFBS, PFHxS, and 6:2 FTS showed likely curvi-linear uptake as little to no increase in mass was exhibited between 16-28 days before increases were observed at 54 days. The apparent reduced uptake of PFAS observed here could be explained by electrostatic repulsion of diffusing compounds within the pore space of the PE membrane once it PFAS have covered its surface (see below). These results suggest that a shorter deployment length of 14 days should be used to ensure all compounds remain in or close to the linear uptake during sampler deployment. For high molecular weight PFSA's like PFHxS, PFHpS, and PFOS, this could explain the discrepancy between field sampling rates being lower than both laboratory and model-derived sampling rates.

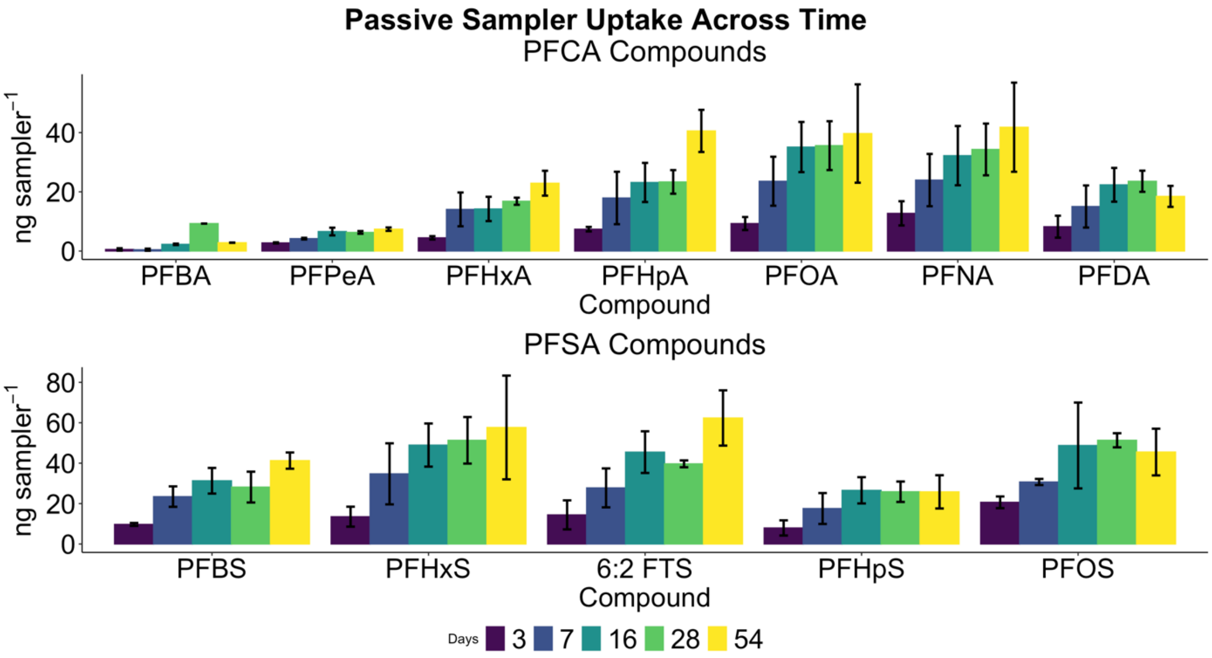

Figure 3. Mean uptake (ng) of PFAS by replicate passive samplers over 3, 7, 16, 28 and 54 days (Error bars are 1 standard deviation).

Sampling Rates of PFAS in the field. PFHxA displayed sampling rates of 40 ±10 mL day^{-1} in the riverine field deployments at >20 cm s^{-1} water velocity for 21-32 days at two temperature profiles, 5 and 15℃ (Table 1). These values are not different given the overlapping uncertainties with the laboratory observed sampling rates (100±81 mL day^{-1}) and model predicted sampling rates (48 ±25 mL day^{-1}). Sampling rates for PFHxS showed slight differences between the field values (50 ±20 mL day^{-1}) and the similar laboratory (120 ±63 mL day^{-1}) and modeled (110 ±53 mL day^{-1}) sampling rates. Field sampling rates could be lower than model or laboratory derived sampling rates due to their longer (14 versus 28-32 day) deployment lengths. Tube passive samplers deployed in the field displayed lower variance than laboratory observed passive samplers with an average standard deviation of 43% in the field replicates compared to 61% in the laboratory. The high variance in the lab measured sampling rates likely reflects the high standard deviation in the lab measured K_{mw} values from the tank experiments (Table S6).

Passive samplers deployed in the field in this experiment exhibited higher sampling rates than those reported by a recent study using this design in waste water treatment plant effluent (Table 1).[44] PFHxA field sampling rates in two high flow rivers reported in this study were 46 ± 40 mL day^{-1} compared to 18 ± 5.5 mL day^{-1} from literature. One explanation could be the low flow, heavily polluted nature of the waste water treatment plant environment suppressing uptake of PFAS (i.e. PFAS were effectively outcompeted) compared to surface waters and experimental lab settings discussed in this study.

Passive samplers deployed in ground water conditions exhibited comparable sampling rates to a previous study using the same tube passive sampler design for PFAS monitoring in groundwater.[24] In this study, sampling rates measured ranged from 1.8 – 3.2 mL day^{-1} for PFBA, PFPeA, PFHxA, PFHpA, and PFOA compared to 2.0-3.0 mL day^{-1} for the same compounds reported by Kaserzon et al. 2019.[24]

Uptake of PFAS by PE Tube. For the parametrization of the uptake model using equation 2, the K_{mw} values are of great importance. Surprisingly, we observed results a difference of almost an order of magnitude between the low flow batch experiment and tank experiment derived K_{mw} values (e.g., for PFOA 0.55 g Water/g HDPE vs 3.5 g Water/g HDPE) (Table S6). In both sets of data the uptake of PFAA by the empty PE tube membranes increased with chain length. PFSA exhibited higher partitioning values between membrane-water phases than their PFCA homologues (Table S6). Published values for PFAA partitioning to PE were limited, though a published value for PFOS partitioning to PE was within 20% of the high flow K_{mw} value for PFOS reported in this study.[48] Diffusion through membrane was calculated to be the largest resistance to uptake between the three phases of this passive sampler design (Fig S7) thus validating the use of this sampling rate model instead of a diffusion model for predicting uptake.[37] We hypothesize that the presence of flow disrupts the water boundary layer significantly, allowing more PFAS compounds to diffuse and adsorb into the interior pore spaces of the membrane. This increase in K_{mw} is significant to the accuracy of the model, as Figure 4 displays that how the predictions of sampling rate from low K_{mw} values better align with our measured groundwater sampling rates as well as previously published samples.[24] Similarly, the higher K_{mw} derived estimates better represent the field and laboratory tank measured sampling rates of this study (Fig 4). However, these higher values from the tank experiments show greater variability and K_{mw} values must be better constrained to improve this model approach going forward. For this reason, we suggest using the tank derived K_{mw} values for surface waters with flow of >0.5 cm s^{-1} and using the batch experiment K_{mw} values for ground water sampling rate predictions.

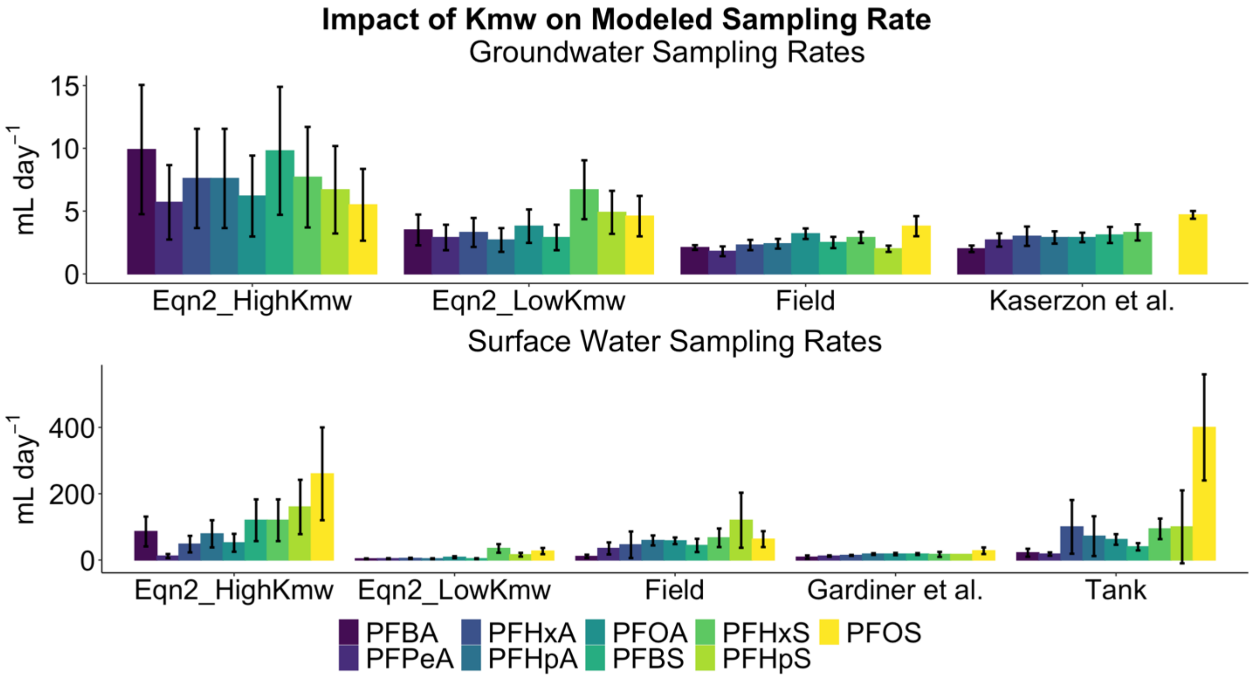

FIGURE 4. Influence of low and high K_{mw} values on equation 2 modeling approach in groundwater and surface water. Error bars display either standard deviation of field/laboratory replicates or uncertainty of the model. Data is included from previous field deployments of this passive sampler design by Kaserzon et al. 2019 in groundwater and Gardiner et al. 2022 in waste water treatment effluent.[24,44]

Uptake of PFAS by sorbent. Uptake of PFAS by the HLB sorbent generally increased with chain length (Table S6) for PFCA and PFSA. Log K_{sw} ranged from 2.7 for C4 (PFBA) to 6.0 for C9 (PFNA) and were in good agreement with previous literature (3.5-5.7).[25] PFSA displayed greater log K_{sw} values than PFCA: 4.8 for PFBS, and a linear increase from PFHxS to PFOS (Log K_{sw} 4.2-5.6) which were also in line with reported values (4.2-5.3 for PFBS, PFHxS, and PFOS)(Table S6).[34] Sorption to HLB was consistent, with an average standard deviation of 3.4%, suggesting that the uptake of PFAS by the HLB sorbent is not a major source of uncertainty in the model derived sampling rate predictions. K_{sw} values were consistently much greater than K_{mw} values, indicating that the HLB sorbent is the main receiving phase for any PFAS taken up by the passive sampler. For future applications, an understanding on how environmental matrices will impact K_{sw} values should be investigated as well.

Comparison to other Passive Samplers for PFAA. The observed PFAS sampling rates were compared to published sampling rates from other integrative passive samplers, normalized to sampler surface area.[20,32,33] The tube passive sampler displayed a surface-normalized sampling rate (Rs/Area, or mass transfer) of almost an order of magnitude higher than the standard POCIS design (Table S5). The mass transfer fell within the ranges reported for DGT samplers, though it was lower than the reported modified POCIS method developed with a smaller surface area (Table S5)

Comparison of two Modeling Approaches for Sampling Rate. The core difference between these two approaches is that equation 2 includes partitioning to the membrane and sorbent, in addition to diffusion, while equation 5 models uptake rates based on diffusion only.

Several lines of evidence imply that sorption to the membrane is important. Both this study and two other studies using this tube sampler design for PFAS display a general increase in sampling rate with chain length (Table 1).[24,44] Equation 2 is impacted by the K_{mw} values used, serving as a modifier that shows an increase in sampling rate with chain length and molecular mass (PFPeA 12 mL day^{-1} to PFOA 52 mL day^{-1} at 15 ℃). An increase in sampling rate from equation 2 compared to the equation 5 model (Fig 4, Table S6) is observed for compounds that exhibit K_{mw} values greater than 1. In contrast, when K_{mw} is less than 1 in the low flow regime, we see a decrease in equation 2 sampling rates relative to equation 5 (Fig 4, Table 1). Taking PFHxS for example, equation 2 predicts a 120 (±63) mL day^{-1} versus 12 (±3.4) mL day^{-1} from equation 5. Equation 5 also shows a decrease in sampling rate with chain length, as partitioning considerations are simplified out of the math, a trend contrary to this study's data and previous publications[24, 44]. Both models do exhibit flow resistance between 0.5-60 cm s^{-1} in modeled sampling rate predictions, indicating that the thickness of the membrane still plays a vital role in both estimates (Fig S4, S5). The propagated error of both models was 52% equation 2 with equation 5 at 29% based off uncertainties in the terms of each model such as K_{mw}, K_{sw}, and diffusivity. These results suggest that equation 5 may be the most appropriate approach for explaining sampling rates, with further refinement necessary.

Comparison of Model, Laboratory, and Field Sampling Rates. Ultimately, equation 2 seem best suited for predicting uptake rates when compared to the field and laboratory data: PFHxA exhibited sampling rates ranged from 37-46 mL day^{-1} at two temperatures in the field, while equation 2 models predicted 35-48 mL day^{-1} (while equation 5 predicted 11-15 mL day^{-1}).

For shorter chain compounds with lower anticipated partitioning to the membrane, equation 5 overestimates sampling rate when compared equation 2 (Table 1). PFBA had field and laboratory Rs values of 11 ($\pm$5.0) and 22 ($\pm$12) mL day $^{-1}$ respectively at 15 ℃, compared to the predictions of 86 $\pm$45 (eqn 5) and 5.1 ± 1.8 mL day^{-1} (eqn 2). This is likely due to overestimated K_{mw} for these shorter, more polar compounds and requires further study. PFHxS displayed field values at 15 ℃ of 67$\pm$28, with modeled sampling rates of 120 ± 63 (eqn 2) and 12 ± 3.4 mL day^{-1} (eqn 5).

Laboratory measured samples rates were anomalously high in comparison to field and both model predictions (Table 1, Fig 1). This is likely because of the lack of environmental matrix, which could compete with PFAS for binding sites on the membrane surface and within the HLB sorbent. In addition, the significant difference we observed in K_{mw} values from either batch or tank experiments seems to suggest that sorption to the membrane can be enhanced in higher-flow environments. PFHxA sampling rates in the laboratory were almost double that of the sampling rates in the field (100 $\pm$81 vs 46 ± 40 mL day^{-1}).

Environmental Implications. In this study, the tube passive sampler was shown to take up PFAA with 4-8 carbon chain lengths in a predictable manner in the field. The resistance to varying water flows exhibited by the tube passive sampler in both the laboratory and model estimations for sampling rates (Fig 1, S4, S5) provided an advantage for widespread deployments in surface waters without the need for site specific calibration. These Rs models can easily be tweaked for temperatures outside of the 15-25 ℃ discussed here, and a predicted sampling rate, or range of sampling rates, can be applied to riverine or estuarine flows >0.5 cm s^{-1}. Further investigation of low flow conditions may be necessary for broad groundwater deployments, though the initial measured sampling rates in groundwater from this study were in good agreement with previously reported data.[24] Overall, the sampler promises to be a simple tool that can be used to screen for PFAS concentrations in environmental waters.

Future work could investigate a sorbent other than HLB might increase sampler uptake over time and reduced the potential matrix effect in environmental waters. Sampling rates for the tube membrane (without sorbent) were lower than all model, field, or laboratory-measured sampling rates for the tube passive sampler, indicating that the membrane is not the major reservoir for PFAS in the sampler (Fig S6). This suggests that the leveling off of uptake exhibited between 16-54 days could be due to sorbent congestion or inefficient transport of PFAS through the membrane layer. The determination of accurate aqueous diffusion coefficients and K_{mw} values for many PFAS compounds is essential to improving the accuracy and application of this work.

Based on the field and laboratory results presented here, we suggest the use of the equation 2's predicted sampling rates for 14-day deployments, while additional work is needed to better constrain the importance of K_{sw} and K_{mw} values within the model estimates. It is clear from this work that K_{mw} is an important term to include in the model to reflect an increase in sampling rate with chain length, making equation 5 a poor choice. However, equation 2 shows high sensitivity to the K_{mw} values, with sampling rates suppressed by K_{mw} lower than 1 in ground water deployments. Future directions should characterize the change in these partitioning values in the presence of environmental matrix, while expanding the number of compounds and methods for PFAS detection that this sampler design is validated for detecting in surface and ground waters.

Associated Content

Supporting Information

The Supporting Information is available free of charge on the ACS Publications website at DOI: It contains additional analytical details, methods, standards, quality control and assurance, LC/MS conditions, details on field deployment sites and conditions, sampling rates for 9 PFAA compounds of interest, images of experimental tank setup and bio fouled passive samplers recovered from the field, interlaboratory comparison data and results.

Author Information

Corresponding Author

Email: rlohmann@uri.edu. Phone (401)874-6612

ORCID

Matthew Dunn: 0000-0002-8902-8434

Jitka Becanova: 0000-0002-3091-1054

Jarod Snook:

Bridger Ruyle: 0000-0003-1941-4732

Rainer Lohmann: 0000-0001-8796-3229

Notes

The authors declare no competing financial interest.

Acknowledgements

The authors acknowledge funding from the Department of Defense’s Strategic and Environmental Research Development Program (Grant # ER18-1280) and the URI STEEP Superfund Research Center (P42ES027706). We thank Denis LeBlanc (USGS), Nicholas Noons and Kirsten Bailey (Rhode Island Department of Environmental Management), Thomas Garrows, Melissa Woodward, Asta Habtemichael, Anna Robuck, and Izak Hill (all URI) for field support, and Dr. Kees Booij (PaSOC) for valuable comments on a previous version of this manuscript.

References

1. Buck, R. C., Franklin, J., Berger, U., Conder, J. M., Cousins, I. T., Voogt, P. de, Jensen, A. A., Kannan, K., Mabury, S. A., & van Leeuwen, S. P. J. (2011). Perfluoroalkyl and polyfluoroalkyl substances in the environment: Terminology, classification, and origins. *Integrated Environmental Assessment and Management*, *7*(4), 513–541. https://doi.org/10.1002/ieam.258
2. Schaider, L. A., Balan, S. A., Blum, A., Andrews, D. Q., Strynar, M. J., Dickinson, M. E., Lunderberg, D. M., Lang, J. R., & Peaslee, G. F. (2017). Fluorinated compounds in U.S. fast food packaging. *Environmental Science and Technology Letters*, *4*(3), 105–111. https://doi.org/10.1021/acs.estlett.6b00435
3. Houtz, E. F., Higgins, C. P., Field, J. A., & Sedlak, D. L. (2013). Persistence of perfluoroalkyl acid precursors in AFFF-impacted groundwater and soil. *Environmental Science & Technology, 47, 8187-8195* https://doi.org/10.1021/es4018877
4. Wang, Z., Dewitt, J. C., Higgins, C. P., & Cousins, I. T. (2017). A Never-Ending Story of Per- and Polyfluoroalkyl Substances (PFASs)? *Environmental Science and Technology*, *51*, 2508–2518. https://doi.org/10.1021/acs.est.6b04806
5. Ojo, A. F., Peng, C., & Ng, J. C. (2021). Assessing the human health risks of per- and polyfluoroalkyl substances: A need for greater focus on their interactions as mixtures. *Journal of Hazardous Materials*, *407,* 124863. https://doi.org/10.1016/j.jhazmat.2020.124863
6. Sunderland, E. M., Hu, X. C., Dassuncao, C., Tokranov, A. K., Wagner, C. C., & Allen, J. G. (2019). A review of the pathways of human exposure to poly- and perfluoroalkyl substances

(PFASs) and present understanding of health effects. *Journal of Exposure Science and Environmental Epidemiology*, *29*(2), 131–147. https://doi.org/10.1038/s41370-018-0094-1

7. Cordner, A., de La Rosa, V. Y., Schaider, L. A., Rudel, R. A., Richter, L., & Brown, P. (2019). Guideline levels for PFOA and PFOS in drinking water: the role of scientific uncertainty, risk assessment decisions, and social factors. *Journal of Exposure Science & Environmental Epidemiology*, *29, 157-171*. https://doi.org/10.1038/s41370-018-0099-9
8. Robuck, A. R., McCord, J. P., Strynar, M. J., Cantwell, M. G., Wiley, D. N., & Lohmann, R. (2021). Tissue-specific distribution of legacy and novel per- and polyfluoroalkyl substances in juvenile seabirds. *Environmental Science and Technology Letters*, *8*(6), 457–462. https://doi.org/10.1021/acs.estlett.1c00222
9. Dassuncao, C., Hu, X. C., Zhang, X., Bossi, R., Dam, M., Mikkelsen, B., & Sunderland, E. M. (2017). Temporal shifts in poly- and perfluoroalkyl substances (PFASs) in north atlantic pilot whales indicate large contribution of atmospheric precursors. *Environmental Science and Technology*, *51*, 4512–4521. https://doi.org/10.1021/acs.est.7b00293
10. Mussabek, D., Ahrens, L., Persson, K. M., & Berndtsson, R. (2019). Temporal trends and sediment–water partitioning of per- and polyfluoroalkyl substances (PFAS) in lake sediment. *Chemosphere*, *227*, 624–629. https://doi.org/10.1016/j.chemosphere.2019.04.074
11. Morales-McDevitt, M. E., Becanova, J., Blum, A., Bruton, T. A., Vojta, S., Woodward, M., & Lohmann, R. (2021). The Air That We Breathe: Neutral and Volatile PFAS in Indoor Air. *Environmental Science & Technology Letters, 8, 897-902*. https://doi.org/10.1021/acs.estlett.1c00481
12. Kannan, K., Corsolini, S., Falandysz, J., Fillmann, G., Kumar, K. S., Loganathan, B. G., Mohd, M. A., Olivero, J., van Wouwe, N., Yang, J. H., & Aldous, K. M. (2004). Perfluorooctanesulfonate and related fluorochemicals in human blood from several countries. *Environmental Science and Technology*, *3*8, 4489–4495. https://doi.org/10.1021/es0493446

13. OECD.org (2021). Portal on Per and Poly Fluorinated Chemicals. *Organization for Economic Co-operation and Development*. https://www.oecd.org/chemicalsafety/portal-perfluorinated-chemicals/countryinformation/european-union.htm#
14. Strong, J. (2016). Lifetime health advisories and health effects support documents for perfluorooctanoic acid and perfluorooctane sulfonate. *Environmental Protection Agency Federal Register 81(101).* https://www.govinfo.gov/content/pkg/FR-2016-05-25/pdf/2016-12361.pdf
15. Cousins, I. T., DeWitt, J. C., Glüge, J., Goldenman, G., Herzke, D., Lohmann, R., Miller, M., Ng, C. A., Scheringer, M., Vierke, L., & Wang, Z. (2020). Strategies for grouping per- and polyfluoroalkyl substances (PFAS) to protect human and environmental health. *Environmental Science: Processes & Impacts*, *22*(7), 1444–1460. https://doi.org/10.1039/d0em00147c
16. Lohmann, R. (2012). Critical review of low-density polyethylene's partitioning and diffusion coefficients for trace organic contaminants and implications for its use as a passive sampler. *Environmental Science and Technology*, *46*(2), 606–618. https://doi.org/10.1021/es202702y
17. Booij K, Vrana B, & Huckins J.N. (2007). Theory, modelling, and calibration of passive samplers used in water monitoring. In Greenwood R, Mills GA, Vrana B, eds, Passive Sampling Techniques in Environmental Monitoring. Elsevier, Amsterdam, The Netherlands, pp 141–169
18. Harman, C., Allan, I. J., & Bäuerlein, P. S. (2011). The challenge of exposure correction for polar passive samplers the PRC and the POCIS. *Environmental Science and Technology*, *45*(21), 9120–9121. https://doi.org/10.1021/es2033789
19. Fauvelle, V., Kaserzon, S. L., Montero, N., Lissalde, S., Allan, I. J., Mills, G., Mazzella, N., Mueller, J. F., & Booij, K. (2017). Dealing with flow effects on the uptake of polar compounds by passive samplers. *Environmental Science and Technology*, *51*(5), 2536–2537. https://doi.org/10.1021/acs.est.7b00558

20. Kaserzon, S. L., Kennedy, K., Hawker, D. W., Thompson, J., Carter, S., Roach, A. C., Booij, K., & Mueller, J. F. (2012). Development and Calibration of a Passive Sampler for Perfluorinated Alkyl Carboxylates and Sulfonates in Water. *Environmental Science & Technology*, *46*(9), 4985–4993. https://doi.org/10.1021/es300593a

21. Kaserzon, S.L., Vermeirssen, E.L.M., Hawker, D.W., Kennedy, K., Bentley, C., Thompson, J., Booij, K., & Mueller, J.F. (2013). Passive sampling of perfluorinated chemicals in water: Flow rate effects on chemical uptake. *Environmental Pollution, 177, 58-63. https://doi.org/10.1016/j.envpol.2013.02.002*

22. Lai, Y.F., Rauert, C., Gobelius, L., & Ahrens, L. (2019) A critical review on passive sampling in air and water for per- and polyfluoroalkyl substances (PFASs). *Trends in Analytical Chemistry, 121, 115-311.* https://doi.org/10.1016/j.trac.2018.11.009

23. Fauvelle, V., Montero, N., Mueller, J. F., Banks, A., Mazzella, N., & Kaserzon, S. L. (2017). Glyphosate and AMPA passive sampling in freshwater using a microporous polyethylene diffusion sampler. *Chemosphere*, *188*, 241–248. https://doi.org/10.1016/j.chemosphere.2017.08.013

24. Kaserzon, S. L., Vijayasarathy, S., Bräunig, J., Mueller, L., Hawker, D. W., Thomas, K. v., & Mueller, J. F. (2019). Calibration and validation of a novel passive sampling device for the time integrative monitoring of per- and polyfluoroalkyl substances (PFASs) and precursors in contaminated groundwater. *Journal of Hazardous Materials*, *366*(September 2018), 423–431. https://doi.org/10.1016/j.jhazmat.2018.12.010

25. Booij, K., Chen, S., & Trask, J. R. (2020). POCIS calibration for organic compound sampling in small headwater streams. *Environmental Toxicology and Chemistry*, *39*(7), 1334–1342. https://doi.org/10.1002/etc.4731

26. Endo, S., & Matsuura, Y. (2019). Mechanistic Model Describing the Uptake of Chemicals by Aquatic Integrative Samplers: Comparison to Data and Implications for Improved Sampler Co

figurations¨. *Environmental Science & Technology, 53, 1482-1489*. https://doi.org/10.1021/acs.est.8b06225

27. Vrana, B., Mills, G., Greenwood, R., Knutsson, J., Svensson, K., & Morrison, G. (2005). Performance optimization of a passive sampler for monitoring hydrophobic organic pollutants in water. *Journal of Environmental Monitoring*, *7*(6), 612–620. https://doi.org/10.1039/b419070j
28. Huckins, J.N., Petty, J., Orazio, C. E., Lebo, J., Clark, R.C., Gibson, V.L., Gala, W.R., & Echols, K.R. (1999). Determination of uptake kinetics (sampling rates) by lipid-containing semipermeable membrane devices (SPMDs) for polycyclic aromatic hydrocarbons (PAHs) in water. *Environmental Science & Technology, 33, 3918-3923. https://doi.org/10.1021/es990440u*
29. Vrana, B., Mills, G. A., Kotterman, M., Leonards, P., Booij, K., & Greenwood, R. (2007). Modelling and field application of the chemcatcher passive sampler calibration data for the monitoring of hydrophobic organic pollutants in water. *Environmental Pollution*, *145*(3), 895–904. https://doi.org/10.1016/j.envpol.2006.04.030
30. Stephens, B. S., Kapernick, A., Eaglesham, G., & Mueller, J. (2005). Aquatic passive sampling of herbicides on naked particle loaded membranes: Accelerated measurement and empirical estimation of kinetic parameters. *Environmental Science and Technology*, *39*(22), 8891–8897. https://doi.org/10.1021/es050463a
31. Booij, K., & Chen, S. (2018). Review of atrazine sampling by polar organic chemical integrative samplers and chemcatcher. *Environmental Toxicology*, *37*(7), 1786–1798. https://doi.org/10.1002/etc.4160
32. Fang, Z., Li, Y., Li, Y., Yang, D., Zhang, H., Jones, K. C., Gu, C., & Luo, J. (2021). Development and applications of novel DGT passive samplers for measuring 12 per- and polyfluoroalkyl substances in natural waters and wastewaters. *Environmental Science and Technology, 55, 9548-9556*. https://doi.org/10.1021/acs.est.0c08092

33. Gobelius, L., Persson, C., Wiberg, K., & Ahrens, L. (2019). Calibration and application of passive sampling for per- and polyfluoroalkyl substances in a drinking water treatment plant. *Journal of Hazardous Materials*, *362*, *230–237.* https://doi.org/10.1016/j.jhazmat.2018.09.005

34. Urik, J., & Vrana, B. (2019). An improved design of a passive sampler for polar organic compounds based on diffusion in agarose hydrogel. *Environmental Science and Pollution Research*, *26, 15273-15284.* https://doi.org/10.1007/s11356-019-04843-6

35. Wang, P., Challis, J. K., Luong, K. H., Vera, T. C., & Wong, C. S. (2021). Calibration of organic-diffusive gradients in thin films (o-DGT) passive samplers for perfluorinated alkyl acids in water. *Chemosphere*, *263*, 128325. https://doi.org/10.1016/j.chemosphere.2020.128325

36. Becanova, J., Saleeba, Z. S. S. L., Stone, A., Robuck, A. R., Hurt, R. H., & Lohmann, R. (2021). A graphene-based hydrogel monolith with tailored surface chemistry for PFAS passive sampling. *Environmental Science: Nano*, *8*(10), 2894–2907. https://doi.org/10.1039/d1en00517k

37. Booij, K. (2021). Passive sampler exchange kinetics in large and small water volumes under mixed rate control by sorbent and water boundary layer. *Environmental Toxicology and Chemistry, 40 (5), 1241-1254.* https://doi.org/10.1002/etc.4989

38. Glanzman, V., Booij, K., Reymond, N., Weyermann, C., & Estoppey, N. (2021). Determining the mass transfer coefficient of the water boundary layer at the surface of aquatic integrative passive samplers. *Environmental Science & Technology*, 56, 6391-6398. https://pubs.acs.org/doi/10.1021/acs.est.1c08088?ref=PDF

39. Morales-McDevitt, M. E., Dunn, M., Habib, A., Vojta, S., Becanova, J., & Lohmann, R. (2022). Poly- and Perfluorinated Alkyl Substances in Air and Water from Dhaka, Bangladesh. *Environmental Toxicology and Chemistry*, *0*(0), 0–2. https://doi.org/10.1002/etc.5255

40. Weber, A.K., Barber, L.B., LeBlanc, D.R., Sunderland, E.M., & Vecitis, C.D. (2017) Geochemical and hydrologic factors controlling subsurface transport of poly- and

perfluoroalkyl substances, Cape Cod, Massachusetts. *Environmental Science & Technology, 51, 8, 4269-4279.* https://doi.org/10.1021/acs.est.6b05573

41. Ruyle, B.J., Pickard, H.M., LeBlanc, D.R., Tokranov, A.K., Thackray, C.P., Hu, C., Vecitis, C.D., & Sunderland E.M. (2021). Isolating the AFFF signature in coastal watersheds using oxidizable PFAS precursors and unexplained organoflouorine. *Environmental Science & Technology*, 55, 6, 3686-3695. https://doi.org/10.1021/acs.est.0c07296
42. Schaefer, C. E., Drennan, D. M., Tran, D. N., Garcia, R., Christie, E., Higgins, C. P., & Field, J. A. (2019). Measurement of Aqueous Diffusivities for Perfluoroalkyl Acids. *Journal of Environmental Engineering*, *145*(11), 06019006. https://doi.org/10.1061/(asce)ee.1943-7870.0001585
43. Reeks, Michael W. (2011) Stokes-Einstein Equation. *Thermopedia*. https://www.thermopedia.com/content/1156/
44. Gardiner, C., Robuck, A., Becanova, J., Cantwell, M., Kaserzon, S., Katz, D., Mueller, J., & Lohmann, R. Field validations of a novel passive sampler for dissolved PFAS in surface waters. *Environmental Toxicology and Chemistry, 41, 10 2375-2385*. https://doi.org/10.1002/etc.5431
45. Qiang, L., Cheng, J., Mirzoyan, S., Kerkof, L.J., & Haggblom, M.M. (2021). Characterization of microplastic-associated biofilm development along a freshwater-estuarine gradient. *Environmental Science & Technology,* 55, 16402-16412. *https://doi.org/10.1021/acs.est.1c04108*
46. Wang, J., Guo, X., and Xue, J. (2021). Biofilm-developed microplastics as vectors of pollutants in aquatic ecosystems. *Environmental Science & Technology*. 55, 12780-12790. https://doi.org/10.1021/acs.est.1c04466
47. Campos Pereira, H., Ullberg, M., Kleja, D. B., Gustafsson, J. P., & Ahrens, L. (2018). Sorption of Perfluoroalkyl substances (PFASs) to an organic soil horizon – Effect of cation

composition and pH. *Chemosphere*, *207*, 183–191. https://doi.org/10.1016/j.chemosphere.2018.05.012

48. Wang, F., Shih, K. M., & Li, X.Y. (2015). The partitioning behavior of perfluorooctanesulfonate (PFOS) and perfluorooctanesulfonamide (FOSA) on micropoplastics. *Chemosphere,* 119, 841-847. https://doi.org/10.1016/j.chemosphere.2014.08.047